Nested Spiral Chirped Waveguide Bragg Gratings for Tunable Dispersion Compensation

Zhenmin Du[(1)], Tingting Zhang[(2)], Zeyu Liu[(1)], Tianjian Zuo[(2)], Hongwei Chen[(1)]

[(1)] Department of Electronic Engineering, Tsinghua University, Beijing, China, chenhw@tsinghua.edu.cn
[(2)] Network Technology Laboratory, Huawei Technologies Co. Ltd., Shenzhen, 518129, China

Abstract *A novel low-loss on-chip optical dispersion compensator based on nested spiral chirped waveguide Bragg gratings is proposed. As a proof-of-concept demonstration, the device achieves 3-nm bandwidth, 1.75-dB loss, and dispersion compensation up to 7.5-km SMF with low group delay ripple less than ±3 ps.*

Introduction

Bandwidth-hungry applications such as cloud computing, online gaming, and streaming media, demand for faster data centre interconnect solution. With single lane rate increasing form 100 Gbps to 200 Gbps, dispersion tolerance of a transmission system is significantly reduced to 1/4. In terms of intensity modulation directed-detection (IMDD), narrower wavelength spacing, maximum likelihood sequence estimation (MLSE), and more powerful forward error correction (FEC) have been proposed to deal with dispersion penalty [1], which yet increase system cost and power consumption. Coherent systems with advanced digital signal processing (DSP) achieve superior performance at the cost of high power consumption. O-band coherent has been proposed to simplify the equalizer for dispersion compensation [2]. However, its ecosystem is not as mature as C band.

With the development of silicon photonics, integrated optical dispersion compensators (ODCs) bringing the advantages of simplified digital equalization and more compact size than traditional dispersion compensation fibre and modules, have become increasingly attractive. Cascaded micro-ring resonators (MRRs) [3-5] and cascaded Mach-Zehnder interferometers (MZIs) [6,7] have been proposed to achieve large dispersion tuning range. However, the bandwidth of single channel is limited and special control circuits are required to obtain the desired frequency response or compensate for the temperature impact, inevitably increasing hardware complexity and power consumption. Recently, on-chip chirped waveguide Bragg gratings (CWBG) have also attracted significant attention from researchers [8-10]. By resorting to silicon nitride waveguides, CWBG with low waveguide loss, large bandwidth and group delay can be realized. Nevertheless, the small dispersion value, limited dispersion tuning range and large group delay ripple (GDR) makes it challenging for practical application to high-speed short-reach optical systems.

In this paper, we propose a compact tunable ODC with low average GDR, low loss, and large bandwidth. Specifically, different spiral CWBGs are integrated in a nested way to minimize the size of the ODC, so that it can be embedded in pluggable optical transceivers. The tunablity is realized by an integrated optical switch selecting the proper CWBG. As a proof-of-concept demonstration, the ODC fabricated on a silicon nitride platform achieves 3-nm bandwidth and 1.75 dB loss. It compensates dispersion up to 7.5-km single-mode fiber (SMF) link with a 5-km granularity, and the corresponding GDRs are ±1.59 ps and ±2.58 ps respectively. It is worthy to note that the bandwidth and tuning range can be further extended by integrating CWBGs with different wavelength ranges and dispersions.

Design rule of the nested spiral CWBG array

The proposed ODC is composed of a spiral CWBG array and optical switch. The CWBGs in the array can have varied dispersion values, lengths, and bandwidths, and are wound in a nested way, which ensures manufacturing stability and achieves more compact size (than traditional separate arrangement) simultaneously.

When designing the nested CWBG array, several factors have to be taken into account. First of all, the gratings should not interfere with each other. Secondly, since the CWBGs are connected with the output ports of optical switch, it is better to align the endpoint positions of all CWBGs. Thirdly, each CWBG with different lengths should be satisfied. The design rule of the nested grating array may be expressed mathematically as:

$$\begin{bmatrix} r_1 & r_2 & \cdots & r_m \\ 0 & r_2 + a & \cdots & r_m + a \\ \vdots & \vdots & \cdots & \vdots \\ 0 & 0 & 0 & r_m + (m-1)a \end{bmatrix} \begin{bmatrix} n_1 \\ n_2 \\ \vdots \\ n_m \end{bmatrix} +$$

$$\begin{bmatrix} d & 2d & \cdots & md \\ 0 & 2d & \cdots & md \\ \vdots & \vdots & \cdots & \vdots \\ 0 & 0 & \cdots & md \end{bmatrix} \begin{bmatrix} \frac{n_1(n_1-1)}{2} \\ \frac{n_2(n_2-1)}{2} \\ \vdots \\ \frac{n_m(n_m-1)}{2} \end{bmatrix} = \begin{bmatrix} \frac{L_1}{\pi} \\ \frac{L_2}{\pi} \\ \vdots \\ \frac{L_m}{\pi} \end{bmatrix} \quad (1)$$

Where the grating length L_i is arranged in a descend order (i.e. L_1 is the longest). r_1 represents the beginning bending radius of the waveguide. a represents the diameter difference between two neighbouring semi-circle waveguides. Therefore, the radius increment d is $a/2$. r_i (i≥2) represents the semi-circular waveguide radius for the first CWBG when the $(i)^{\text{th}}$ CWBG starts to being wound jointly. After n_i semi-circular waveguides, the (i+1)$^{\text{th}}$ CWBG starts to join. With this principle, we can achieve when m≥2

$$r_m = r_1 + n_1 d + \cdots + n_{m-1} \cdot (m-1)d. \quad (2)$$

The only unknown parameters n_1 to n_m are solvable for the m-dimensional and invertible matrix in Eq. (1). This means that the arrangement of any grating array with varied grating number and length can be determined using Eq. (1).

ODC design and fabrication

The aforementioned design principle applies to any spiral CWBG array. As a proof-of-concept demonstration, we only consider the simplest case (i.e. two CWBGs) in this paper. As shown in Fig. 1, the ODC consists of an optical switch and two spiral CWBGs, which are integrated in a nested way but do not interfere with each other. The entire device is etched and processed on a 90 nm-thick silicon nitride substrate. In order to effectively increase the aspect ratio of the waveguide while ensuring single-mode condition, the waveguide width w_0 is set to 2.8 μm.

The optical switch performs dispersion tunability by selecting the proper output port connected with the desired CWBG. It uses a typical MZI structure with one input port (port in) and two output ports (port out1 and port out2). In our scheme, the electrodes are placed on both the upper and lower arms of the MZI. This allows less power consumption than single electrode MZI, due to smaller phase change required for the waveguide to achieve state switching.

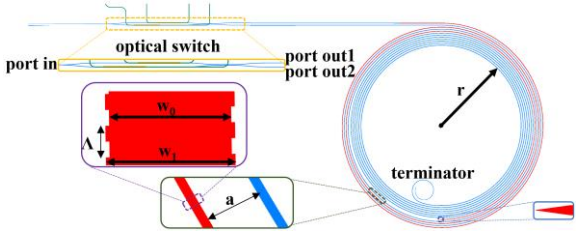

Fig. 1: Schematic diagram of the ODC. The shorter and longer gratings are labelled in red and blue respectively.

Both CWBGs in the array are apodized by a hyperbolic tangent function, and constructed from semi-circular waveguides that are continuously wound into a spiral shape. The spiral waveguide spacing a is 20 μm. To minimize the bending loss of the waveguide, the minimum bending radius r is set to 800 μm. The refractive index periodicity of the grating is achieved by introducing periodic rectangular perturbations on the sidewalls of the waveguide. The waveguide width at the wider sections of the grating is denoted as w_1 (2.8 μm to 2.97 μm) (see Fig. 1). Therefore, the refractive index modulation depth of the grating is (w_1-w_0)/2. The chirp of the grating is achieved by linearly varying the grating period Λ (527.5 nm to 528.9 nm). In order to prevent the reflection of light outside of the bandwidth from adversely affecting the performance of the grating, a terminator is placed at the starting end of each grating to dissipate the transmitted light and prevent it from being reflected back.

Results and discussion

Fig. 2(a) illustrates the microscopic image of the two main components of the device, i.e. the optical switch and the nested CWBG array with an observed largest diameter of 2.04 mm. If the two gratings are arranged separately, the overall size of the grating array will increase from current 3.27 mm² to 5.35 mm². This leads to processing instability and decreased integration of the entire device. The measured transmission spectrum of the optical switch in Fig. 2(b) shows that the switch contrast reaches beyond 20 dB for 30-nm bandwidth (1535 nm to 1565 nm). It should be

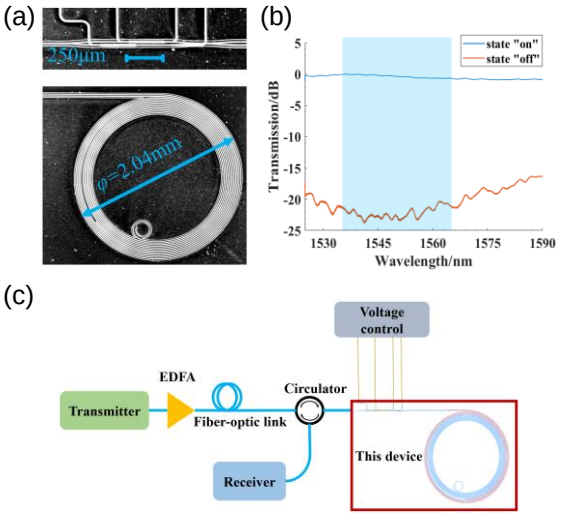

Fig. 2: (a) Microscopic image of the optical switch and CWBG array. (b) Transmission spectrum of the optical switch in "on" and "off" states. (c) Experimental setup for the proposed ODC measurement.

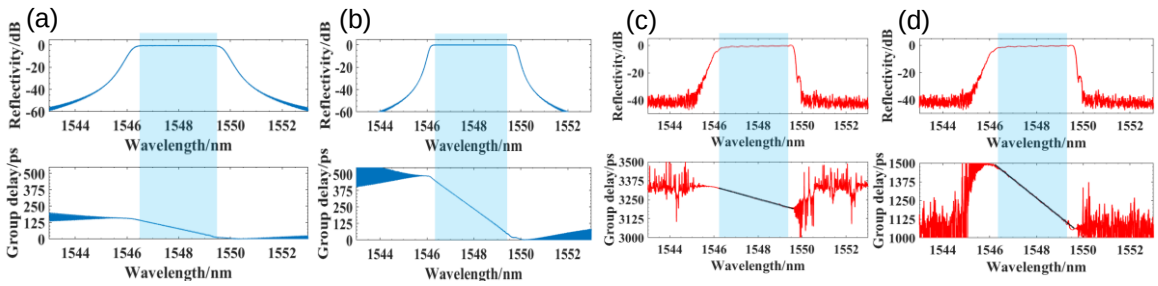

Fig. 3: Simulation results, the reflection spectrum and group delay curve of (a) *gra1* and (b) *gra2*. Experimental results, the measured reflection spectrum and group delay for (c) *gra1* and (d) *gra2*.

noted that since the reflective CWBG is connected after the switch, the input light enters the optical switch, reflects back after two passes, and helps further increase the contrast between different channels. This effectively avoids crosstalk between adjacent channels. The power consumption of the ODC only comes from the optical switch, where each TiN electrode with a resistance of 800 Ω consumes 160 mw to generate a π/2 phase change.

Fig. 3 compares the experimental and simulation results of the two passive CWBGs (*gra1* and *gra2*) with lengths of 1.22 cm and 3.66 cm, respectively. We can observe that the experimental results of the device are in good agreement with the simulation results. As shown in Fig. 3(c) and Fig. 3(d), the working bandwidth of both gratings ranges from 1546.4 nm to 1549.4 nm, as expected. It is also in good agreement with our theoretical calculation. The dispersion for the two gratings, obtained from the group delay slope, are -40.5 ps/nm and -126.45 ps/nm respectively, corresponding to compensate about 2.5km and 7.5km SMF link.. The slight but acceptable difference from simulated dispersion is attributed to the errors in the waveguide group refractive index. On the group delay curve of the gratings, a black line represents the pre-set ideal group delay curve. The average error between the measured group delay curve and the ideal group delay curve gives respective GDR of ±1.59 ps and ±2.58 ps for *gra1* and *gra2*. To the best of our knowledge, the achieved GDR is the smallest by far, in the case of the same CWBG length.

Tab.1 compares our scheme with other works on the integrated dispersion compensator. It can be seen that the proposed scheme exhibits advantages in terms of dispersion tunability, bandwidth, group delay, bandwidth delay product (BDP) and GDR.

Conclusions

An on-chip ODC based on optical switch and nested CWBG array with mathematically expressed design principle is presented in this paper. Dispersion adjustment is achieved by optical switch routing. A proof-of-concept demonstration is carried out by winding two CWBGs with dispersion values of -40.5 ps/nm and -126.45 ps/nm in parallel. This allows 38.9% area reduction, compared with separate arrangement. The measured GDR of the two gratings are ±1.59 ps and ±2.58 ps for 3-nm bandwidth. This entire device is 1.75 dB loss. The bandwidth and dispersion tuning range of the ODC can be further extended by integrating CWBGs with varied wavelength range and dispersion. The reported results are encouraging for the future application to high-speed pluggable optical modules.

Acknowledgements

This work was supported by the National Natural Science Foundation of China (62135009).

Tab. 1: Comparison between this work and previous research.

Index	Bandwidth (nm)	Maximum group delay (ps)	Maximum dispersion (-ps/nm)	Bandwidth Delay Product (ps•nm)	GDR (±ps)	Tunability
[3]	0.4	68	170	27.2	NA	✓
[4]	0.2	144	720	28.8	NA	✓
[5]	0.4	70	175	28	NA	✓
[7]	0.12	66	550	7.92	NA	✓
[10]	1.36	199	146	270.64	13.9	×
This work	**3**	**380**	126.45	**1140**	**1.59/2.58**	✓

References

[1] https://www.ieee802.org/3/df/public/22_11/index.html.

[2] Y. Xia, L. Valenzuela, A. Maharry, S. Pinna, S. Dwivedi, T. Hirokawa, J. Buckwalter, and C. Schow, "A Fully Integrated O-band Coherent Optical Receiver Operating up to 80 Gb/s," in *IEEE Photonics Conference (IPC)*, Vancouver, BC, Canada, 2021, DOI: 10.1109/IPC48725.2021.9592881

[3] M. S. Alam, M. Morsy-Osman, K. A. Shahriar, E. El-Fiky, S. Lessard, G. De Angelis, V. Sorianello, F. Fresi, F. Cavaliere, L. Potì, M. Midrio, M. Romagnoli, G. Vall-Llosera, and D. V. Plant, "224 Gb/s Transmission over 10 km of SMF at 1550 nm Enabled by a SiN Optical Dispersion Compensator and Stokes Vector Direct Detect Receiver", in *OSA Advanced Photonics Congress* Washington, DC United States, 2020, pp. SpM4I.5, DOI: 10.1364/SPPCOM.2020.SpM4I.5

[4] Y. Liu, L. Lu, Z. Ni, J. Chen, J. Chen and L. Zhou, "Silicon Integrated Continuously Tunable Dispersion Compensator Based on Cascaded Micro-Ring Resonators", in *Asia Communications and Photonics Conference (ACP)*, Shenzhen, China, 2022, pp. 1352-1355, DOI: 10.1109/ACP55869.2022.10088552

[5] V. Sorianello, G. De Angelis, F. Fresi, F. Cavaliere, L. Potì, M. Midrio, and M. Romagnoli, "100Gb/s PolMux-NRZ Transmission at 1550nm over 30km Single Mode Fiber Enabled by a Silicon Photonics Optical Dispersion Compensator", in *Optical Fiber Communication Conference*, OSA Technical Digest (online) , San Diego, California United States, 2018, pp. W2A.31, DOI: 10.1364/OFC.2018.W2A.31

[6] R. Moreira, S. Gundavarapu, and D. J. Blumenthal, "Programmable eye-opener lattice filter for multi-channel dispersion compensation using an integrated compact low-loss silicon nitride platform," *Opt. Express*, vol. 24, no. 15, pp. 16732-16742, 2016, DOI: 10.1364/OE.24.016732

[7] G. M. Brodnik, C. Pinho, F. Chang, and D. J. Blumenthal, "Extended reach 40km transmission of C-band real-time 53.125 Gbps PAM-4 enabled with a photonic integrated tunable lattice filter dispersion compensator," in *Optical Fiber Communications Conference and Exposition (OFC)*, San Diego, CA, USA, 2018, pp. 1-3, DOI: 10.1364/ofc.2018.w2a.30

[8] Y. Sun, D. Wang, C. Deng, M. Lu, L. Huang, G. Hu, B. Yun, R. Zhang, M. Li, J. Dong, A. Wang, and Y. Cui, "Large Group Delay in Silicon-on-Insulator Chirped Spiral Bragg Grating Waveguide", *IEEE Photonics Journal*, vol. 13, no. 5, pp. 1-5, 2021, DOI: 10.1109/jphot.2021.3112719

[9] Z. Du, C. Xiang, T. Fu, M. Chen, S. Yang, J. E. Bowers, and H. Chen, "Silicon nitride chirped spiral Bragg grating with large group delay", *APL Photonics*, vol. 5, no. 10, pp. 101302, 2020, DOI: 10.1063/5.0022963

[10] B. Stern, H. Chen, K. Kim, and N. K. Fontaine, "Large Dispersion Silicon Bragg Grating for Full-Field 40-GBd QPSK Phase Retrieval Receiver", *Journal of Lightwave Technology*, vol. 40, no. 22, pp. 7358-7363, 2022, DOI: 10.1109/jlt.2022.3202086